Seasonal influenza circulation patterns and projections for February 2024 to February 2025

John Huddleston[1], Trevor Bedford[1,2], Jennifer Chang[1], Jover Lee[1] & Richard A. Neher[3]

[1]Vaccine and Infectious Disease Division, Fred Hutchinson Cancer Center, Seattle, WA, USA, [2]Howard Hughes Medical Institute, Seattle, WA, USA, [3]Biozentrum, University of Basel, Basel, Switzerland

March 20, 2024

Abstract

This report details current seasonal influenza circulation patterns as of early February 2024 and was prepared for the Northern Hemisphere VCM on Feb 15, 2024. This is not meant as a comprehensive report, but is instead intended as particular observations that we've made that may be of relevance. Please also note that observed patterns reflect the GISAID database and may not be entirely representative of underlying dynamics. Influenza circulation as well as surveillance continues to be strongly affected by our response to the SARS-CoV-2 pandemic over the past three years. Data are hence expected to be biased and predictions particularly uncertain. All analyses are based on the nextflu/nextstrain pipeline [1, 2] with continual updates posted to nextstrain.org/flu. *In compliance with data sharing agreements, this public version of the report does not include raw serological measurements.* **A/H1N1pdm:** H1N1pdm sequence counts have grown rapidly in the last two months in Europe and North America. HA clades C.1, C.1.1.1, and C.1.7 compete regionally without a clear forerunner. C.1's recent success in Europe appears driven by its NA clade C.5 with NA:S200N substitution. C.1.1.1 and C.1.7 continue to diversify and circulate outside of their original dominant countries (USA and Australia). Recurrent substitutions appear at HA1 sites 120, 142, and 152 across most recent clades, but none of these appear associated with antigenic drift. Ferret serology suggests that the current vaccines, A/Wisconsin/67/2022 and A/Sydney/5/2021, cover all extant clades. Human serology based on recent vaccination with A/Wisconsin/588/2019 also shows little antigenic drift for any clades. **A/H3N2:** H3N2 counts are growing rapidly in West Asia and Europe, after a quiet 2023. Clade H has likely fixed globally and has diversified into four new clades H.1, H.2, H.3, and H.4. H.2 has circulated at the highest frequency potentially due to its loss of a glycosylation site at HA1:122 and an antigenic escape substitution at HA1:276E. Ferret serology suggests that H.2 maybe drifted from the H-descendant vaccine A/Massachusetts/18/2022, while A/Darwin/6/2021 continues to cover recent H strains. Human serology also suggest that vaccination with A/Darwin/6/2021 may protect against recent H strains. **B/Vic:** In the last six months, B/Victoria has been sequenced primarily in North America. Sequence counts remain relatively low compared to the peak season in Europe last February and March. Clade C.5 has nearly fixed globally and diversified into subclades including several with recurrent HA1:197E and HA1:183K substitutions. The current vaccine strain, B/Austria/1359417/2021 (basal in C), continues to effectively cover clade C strains observed in the last year.

Contents

Methods and Notes

Sequence data and subsampling

We base our analysis on sequence data available in GISAID as of February 15, 2024 and titer data available as of February 15. The availability of sequences varies greatly across time and geography and we try to minimize geographical and temporal bias by subsampling the data or analyzing different geographical regions separately when appropriate. While this subsampling reduces geographical biases, it doesn't remove this bias entirely.

Phylogenetic analysis

The database contains too many sequences to perform a comprehensive phylogenetic analysis of all available data. We hence subsample the data to at least 3000 sequences collected in the last 2 years. To minimize bias from differences in surveillance intensity, we evenly sample at most 2700 sequences (90%) across region, year and month bins for regions including North America, Oceania, China, South America, West Asia, Japan and Korea, Southeast Asia, Africa, and South Asia. For European data, we sample at most 300 sequences (10%) across country, year and month bins. Within each region/country, year, and month group, we prioritize sequences with corresponding antigenic data. For phylogenetic context, we include an additional 300 sequences collected prior to 2 years ago and as early as January 2016, evenly sampling by region and year. We also include all strains with titer measurements as a test or reference virus, to ensure that all titer data are available to observe in our interactive reports.

Parallel evolution, that is repeated occurrence of identical substitutions in different clades of the tree, is common in A/H3N2 and A/H1N1pdm. Such parallel evolution violates fundamental assumptions of common phylogeny software and can erroneously group distinct clades together if they share too many parallel changes. To avoid such artifacts, we mask sites with rampant parallelism prior to phylogeny inference.

Clades and subclades are assigned using a collection of "signature" mutations available at the GitHub repository github.com/nextstrain/seasonal-flu for each lineage via the following links:

- H1N1pdm HA
- H1N1pdm NA
- H3N2 HA
- H3N2 NA
- Vic HA
- Vic NA

Clade and mutation frequency estimates

Although phylogenetic analyses require a subset of all available sequences to produce an unbiased tree, we apply a non-phylogenetic method to estimate clade and mutation frequencies from all hemagglutinin (HA) sequences per lineage. We align all HA sequences to the lineage's reference sequence using Nextclade and obtain clade labels and amino acid substitutions per sequence [3]. From these Nextclade annotations per sequence, we estimate the frequencies of each clade or amino acid substitution per geographic region in 14-day intervals using a smoothing algorithm that prevents frequencies from

changing too rapidly between adjacent timepoints. We calculate confidence intervals for each frequency trajectory through time that reflect the sampling intensity at each timepoint. See our technical note on this method for more details.

Antigenic analysis

We summarize HI and FRA measurements provided by the WHO CCs in London, Melbourne, Atlanta, and Tokyo using our *substitution model* [4] which models log-titers as a sum of effects associated with amino acid differences between the sequences of the test and reference virus. In addition, the model allows for a serum (column) and a virus (row) effect. This model allows inference of titers for virus/serum pairs that have not been antigenically characterized and isolates effects consistently observed across many measurements from the noise inherent in individual measurements. We also plot individual and average normalized $\log_2$ titers per reference serum for test viruses in specific clades, to represent the raw antigenic data available for each influenza lineage.

Fitness estimates

We estimated the fitness of currently circulating strains using the local branching index (LBI) [5] and estimates of antigenic novelty based on titer measurements from ferret or pooled human sera [6]. High LBI values indicate clades in a phylogeny that have likely experienced recent population growth. High antigenic novelty indicates groups of viruses that are antigenically distant from viruses that have circulated in the last 5 years.

Overall circulation patterns

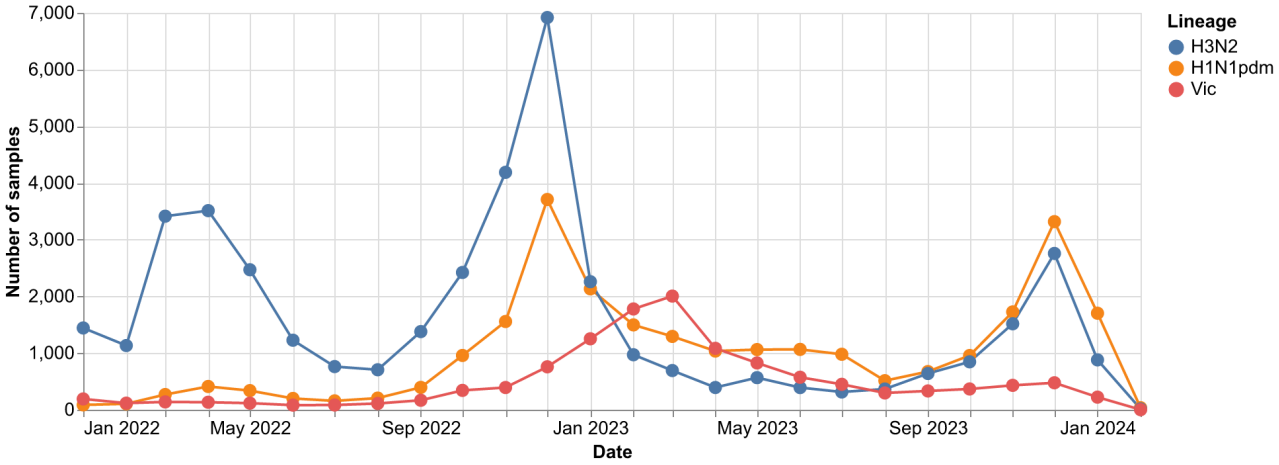

Figure 1. Total genome samples per lineage since January 2022. Recent counts of A/H1N1pdm and A/H3N2 have increased towards the end of 2023, but B/Vic observations remain rare.

A/H1N1pdm

H1N1pdm sequence counts have grown rapidly in the last two months in Europe and North America. HA clades C.1, C.1.1.1, and C.1.7 compete regionally without a clear forerunner. C.1's recent success in Europe appears driven by its NA clade C.5 with NA:S200N substitution. C.1.1.1 and C.1.7 continue to diversify and circulate outside of their original dominant countries (USA and Australia). Recurrent substitutions appear at HA1 sites 120, 142, and 152 across most recent clades, but none of these appear associated with antigenic drift. Ferret serology suggests that the current vaccines, A/Wisconsin/67/2022 and A/Sydney/5/2021, cover all extant clades. Human serology based on recent vaccination with A/Wisconsin/588/2019 also shows little antigenic drift for any clades.

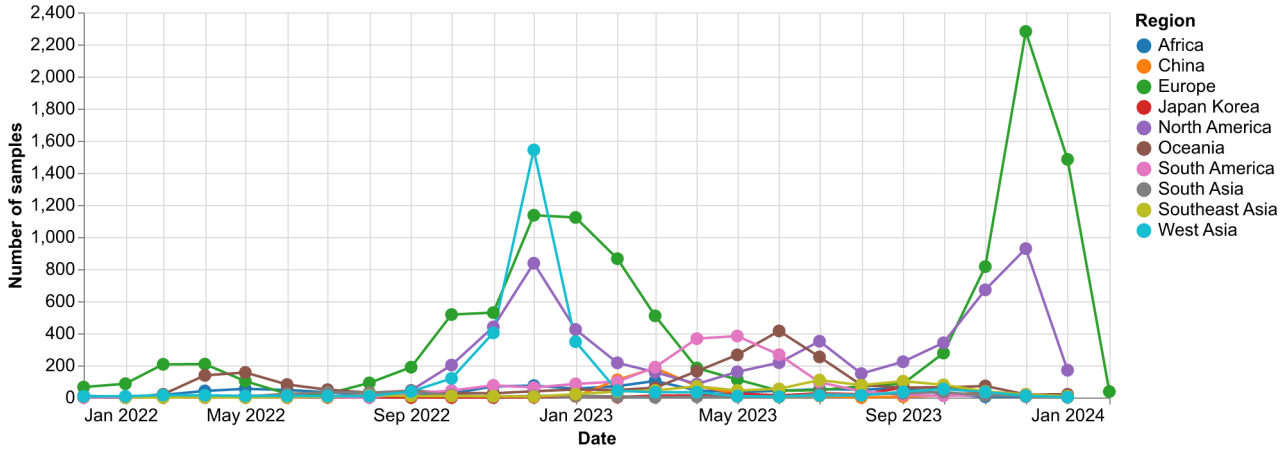

Figure 2. Sample counts through time and across regions.

Current circulation patterns

H1N1pdm sequence counts are higher than they've been since the pandemic (Fig. 1), with the recent increase driven by circulation in Europe and North America (Fig. 2). Among HA clades, C.1 dominates in most regions except Oceania where C.1.7 dominates and North America where C.1.1.1 continues to circulate at the highest frequency (Figs. 3 and 4). The recent growth of C.1 in Europe and North America (Fig. 4) corresponds to the growth of the NA clade C.5 with a S200N substitution (Fig. 5). Note that these NA from clade C.5 are identical to C.5.3 at the amino acid level. The same NA clade is growing slowly in West Asia and South Asia. In contrast, the HA clade C.1 without the NA C.5 clade has been replaced in Japan and Korea by HA clade C.1.1.1.

Since June 2023, the HA clade C.1.1.1 has grown in Japan, Korea, Oceania, and South America (Fig. 4). This clade comprises one subclade with a HA1:45K substitution (circulating mostly in the USA) and another with a HA1:113K substitution (circulating mostly in Japan). HA clade C.1.7 remains at highest frequency in Oceania, but it has grown recently in Japan and Korea, Southeast Asia, and somewhat in North America. We also observed the following recurrent substitutions across clades:

- HA1:120A in C.1, C.1.1.1, and C.1.7
- HA1:142R in C.1, C.1.1, and C.1.7

- HA1:152I in C.1, C.1.3, and C.1.7

However, we did not see strong signals of antigenic drift associated with any of these substitutions in ferret or human serology data.

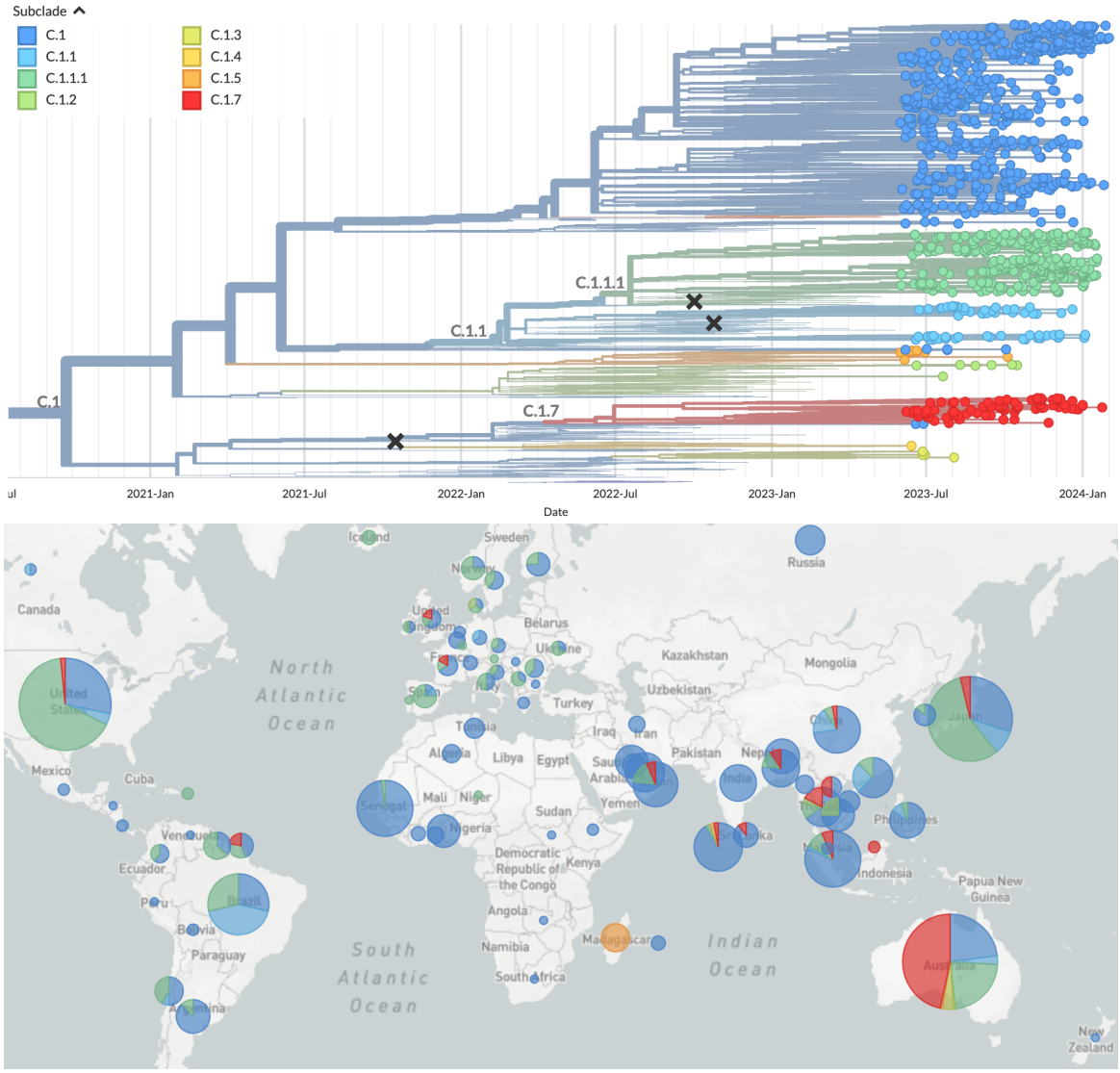

Figure 3. Time-resolved A/H1N1pdm phylogeny colored by clade and filtered to strains collected since June 1, 2023 (top) and corresponding geographic distribution of strains shown in the phylogeny (bottom). View on nextstrain.org.

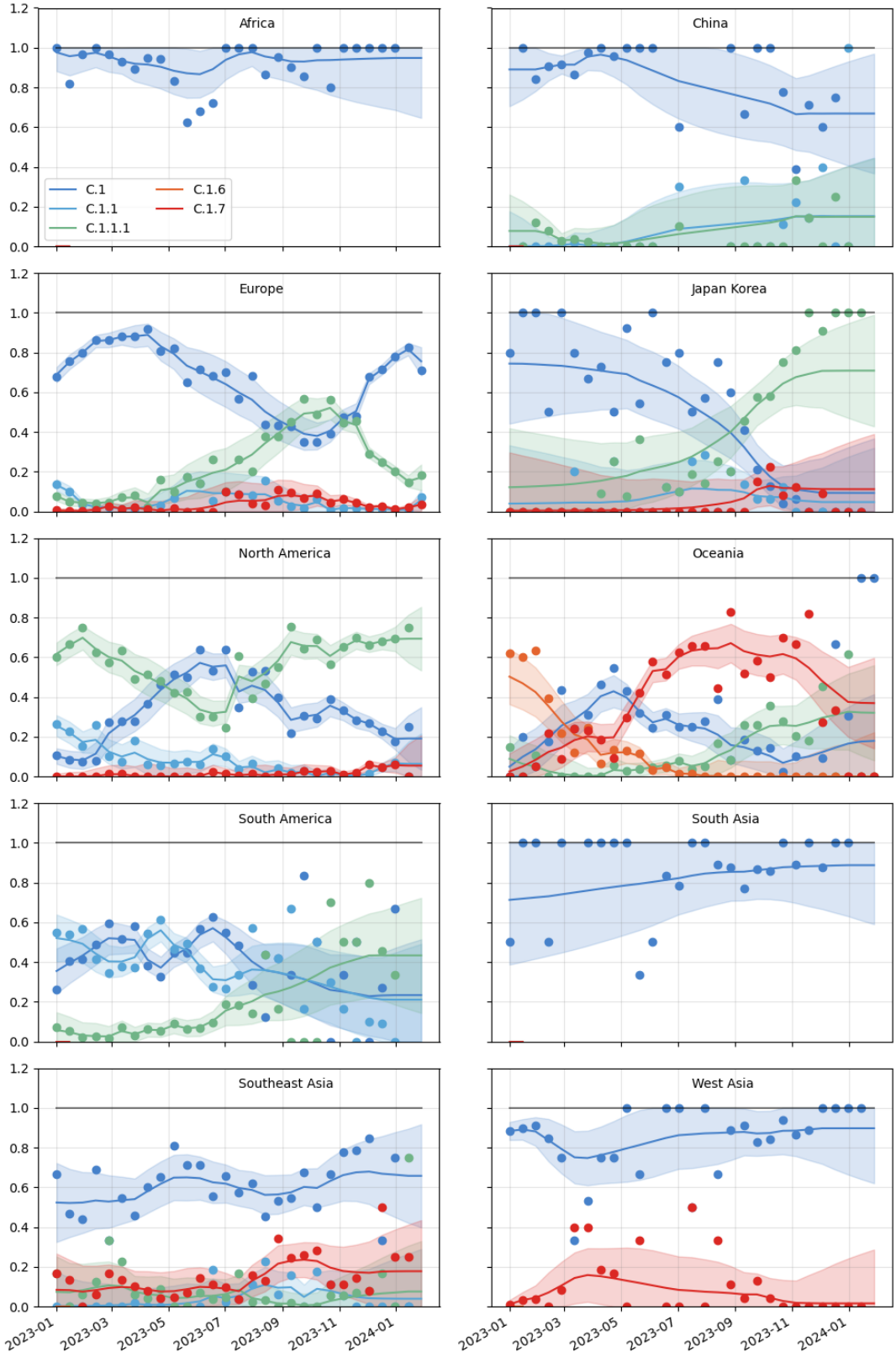

Figure 4. HA clade frequency dynamics in different regions of the world.

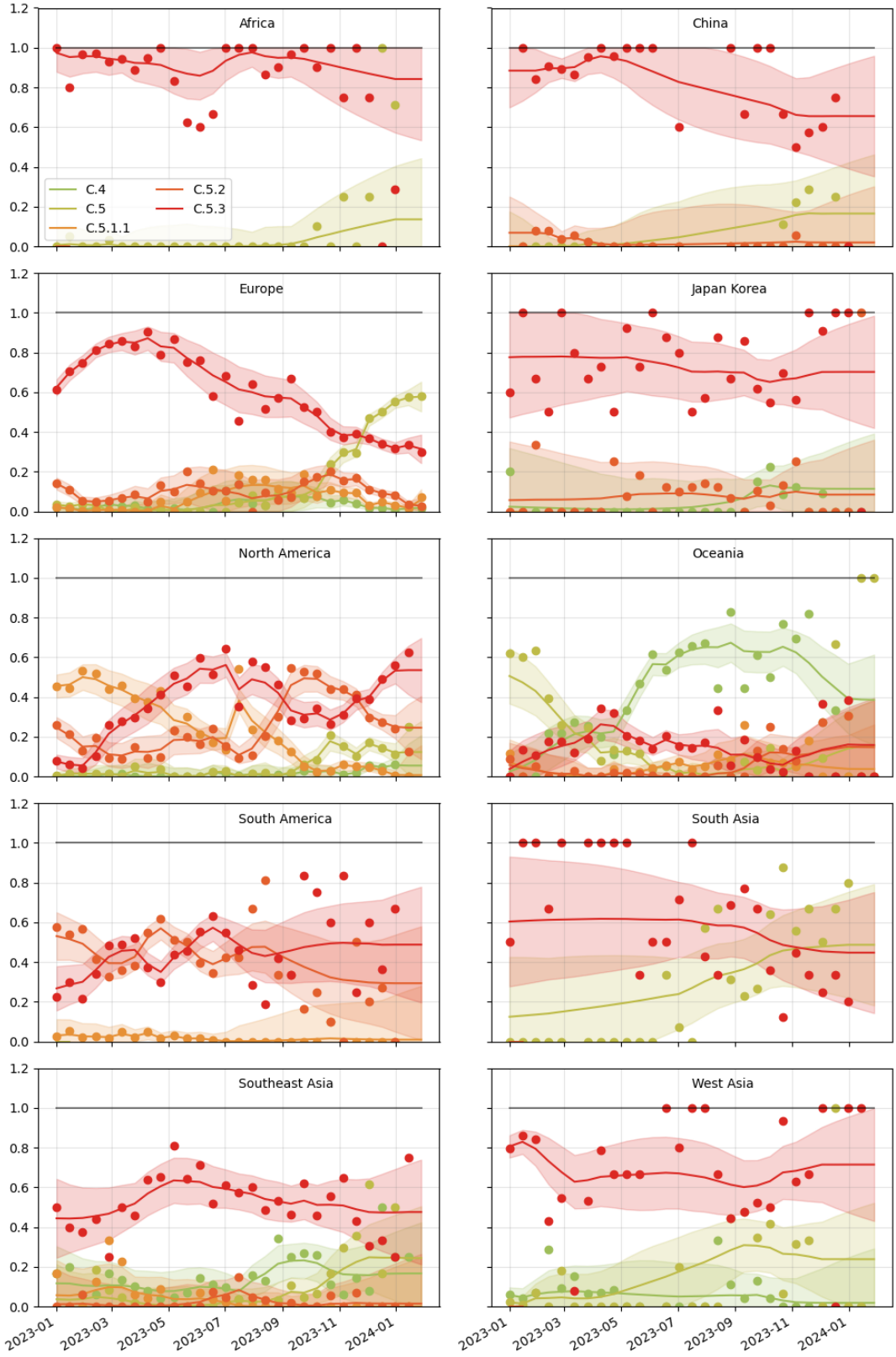

Figure 5. NA clade frequency dynamics in different regions of the world.

Antigenic properties from ferret serology

We aggregated HI data from the WHO Collaborating Centers in London, Tokyo, Melbourne, and Atlanta. The current northern hemisphere cell-based vaccine, A/Wisconsin/67/2022, appears to effectively cover all recent clades. The egg-based vaccine strain, A/Victoria/4897/2022, also covers C.1, C.1.1, and C.1.1.1 but appears less effective against other recent clades. The current southern hemisphere vaccine, A/Sydney/5/2021, effectively covers recent clades similarly in both cell- and egg-passaged formats.

Antigenic properties from pooled human sera

To estimate the effects of recent mutations on human immune responses, we plotted titer measurements from pooled human sera against recently circulating test viruses using the Nextstrain measurement panel [7]. Sera came from humans who had been recently vaccinated with a cell-passaged A/Wisconsin/588/2019 strain in either 2021/2022 or 2022/2023 seasons. Prior to plotting, we filtered test virus measurements to descendants of clade C.1 (5a.2a) that were collected since June 1, 2023, grouped measurements by serum id (reflecting the year the experiments were performed), and colored measurements by clade. Although we previously observed slight antigenic drift of C.1.1 (5a.2a.1) relative to post-vaccination sera in the 2021/2022 season, we do not see the same pattern in data from the 2022/2023 season.

Fitness estimates

C.1.1.1 had the highest novelty of recent clades circulating at global frequencies greater than 5% (Fig. 6). A subset of recent strains from C.1.7 carrying HA1 substitutions 152I, 142R, and 271S showed higher novelty than C.1.1.1, but the rest of C.1.7 had lower novelty on average. Despite high antigenic novelty of C.1.3, this clade has not been observed since August 2023 (Fig. 3). In contrast, clade C.1 has the highest local branching index (LBI) of all clades followed closely by C.1.1.1 and distantly by C.1.7 (Fig. 7). The high LBI of HA clade C.1 corresponds to a part of the clade without any characteristic HA1 substitutions driven by dense sampling in Europe. However, this clade's corresponding NA clade C.5 carries two substitutions (469N and 200N) and has grown rapidly in frequency, suggesting that the recent success of the HA C.1 clade is caused by the success of its NA.

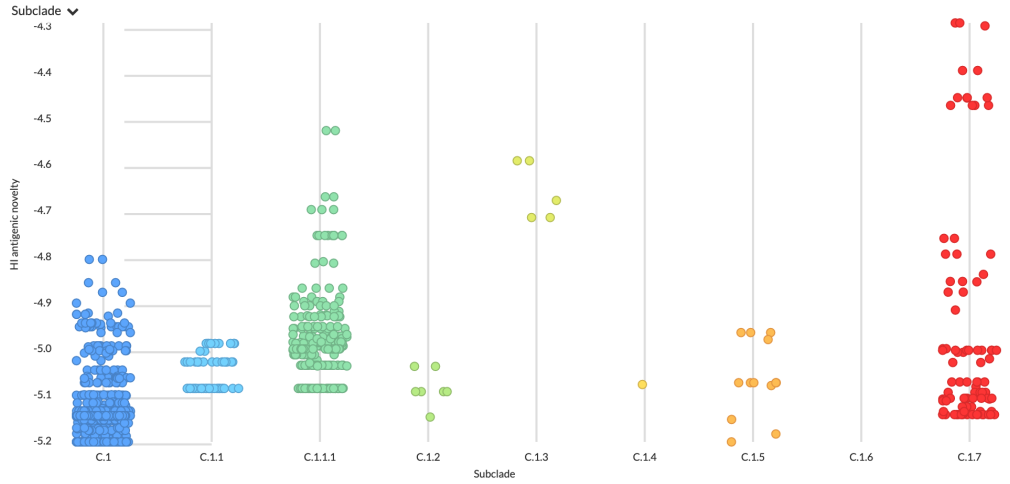

Figure 6. Antigenic novelty per clade estimated from ferret-based HI data [6] for samples collected since June 1, 2023. View on nextstrain.org.

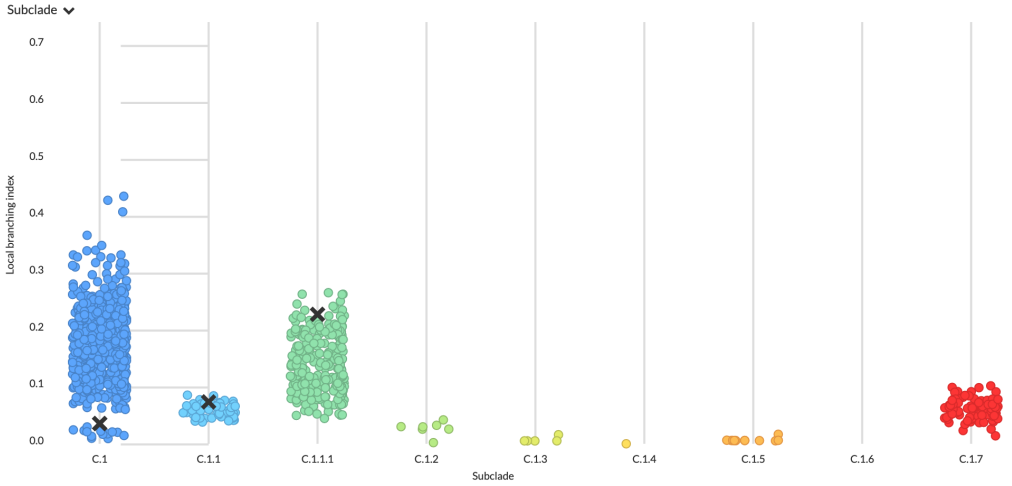

Figure 7. Local branching index per clade [5] for samples collected since June 1, 2023. View on nextstrain.org.

A/H3N2

H3N2 counts are growing rapidly in West Asia and Europe, after a quiet 2023. Clade H has likely fixed globally and has diversified into four new clades H.1, H.2, H.3, and H.4. H.2 has circulated at the highest frequency potentially due to its loss of a glycosylation site at HA1:122 and an antigenic escape substitution at HA1:276E. Ferret serology suggests that H.2 maybe drifted from the H-descendant vaccine A/Massachusetts/18/2022, while A/Darwin/6/2021 continues to cover recent H strains. Human serology also suggest that vaccination with A/Darwin/6/2021 may protect against recent H strains.

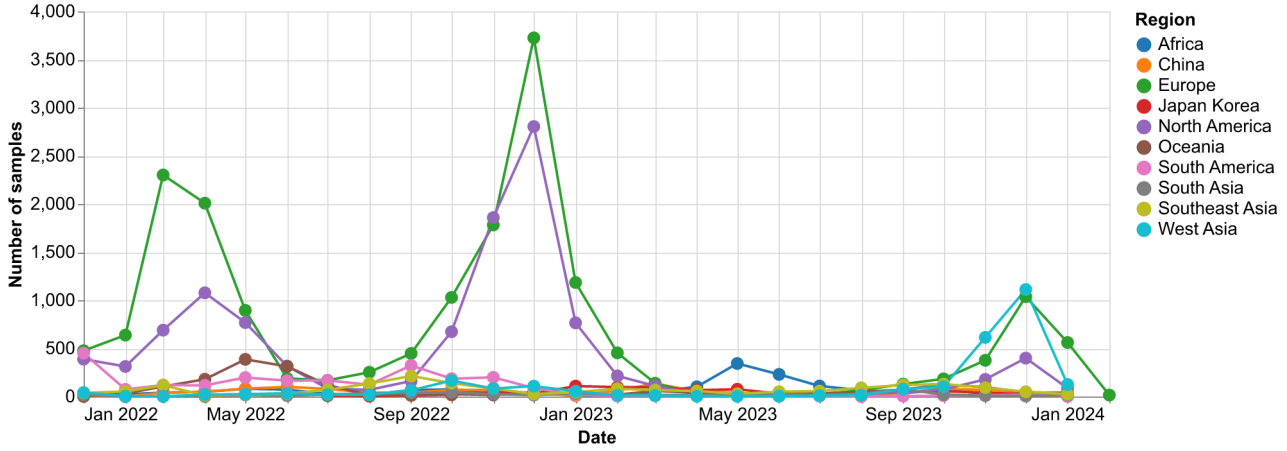

Figure 8. Sample counts through time and across regions.

Current circulation patterns

After a year of low H3N2 HA sequence counts, the total HA sequences per month has increased in the last two months (Fig. 1) with most sequences collected in West Asia, Europe, and North America (Fig. 8). During these two months, the clade H has effectively fixed (Fig. 10) and continued to diversify (Fig. 9). We note four new subclades of clade H including:

H.1: HA1:25V, HA2:V18M, and circulating with NA:331G and NA:26T (Fig. 12)

H.2: HA1:122D and HA1:276E

H.3: HA2:176I

H.4: HA1:173R and HA1:276E

H.1 and H.2 represent the majority of recent H sequences (Fig. 10). Both clades have cocirculated in Europe, North America, Oceania, and West Asia in the last 6 months. H.2 appears at equal or higher frequencies than H.1 in all of these regions and appears to be fixing in West Asia. H.2's success may be associated with the fact that its HA1:N122D substitution removes a glycosylation site and its HA1:K276E substitution occurs at a putative epitope site. HA1:122D remained at low frequencies after it emerged in the middle of 2022 and until after HA1:276E occurred sometime between December 2022 and April 2023 (Fig. 13). In contrast to H.2, H.1 is only dominant in the Japan/Korea region. There are few recent sequences from Africa, China, South America, or South Asia, so we are most likely underestimating the diversity of H3N2 HA clades circulating in these populous regions. In addition to

the clades noted above, we also observe at least 15 independent recurrent HA1:S145N substitutions throughout clade H. This substitution adjacent to the receptor binding site remains at low frequencies globally, but it may be growing in Oceania (Fig. 14). We also observe several independent recurrent HA1:K189R substitutions throughout clade H. The most notable emergence is in H.4 and comprises 30 sequences mostly from West Africa with some observations from Europe (Fig. 15).

In the NA segment, clade B.4 has fixed along with HA subclade H (see Fig. 11). The NA subclade B.4 has diversified and HA subclades H.1 and H.2 are associated with distinct subclades in NA (Fig. 12). Another recent cluster in subclade H.2 with sequences from Idaho, Norway, and England combine the 145N and 189R substitutions.

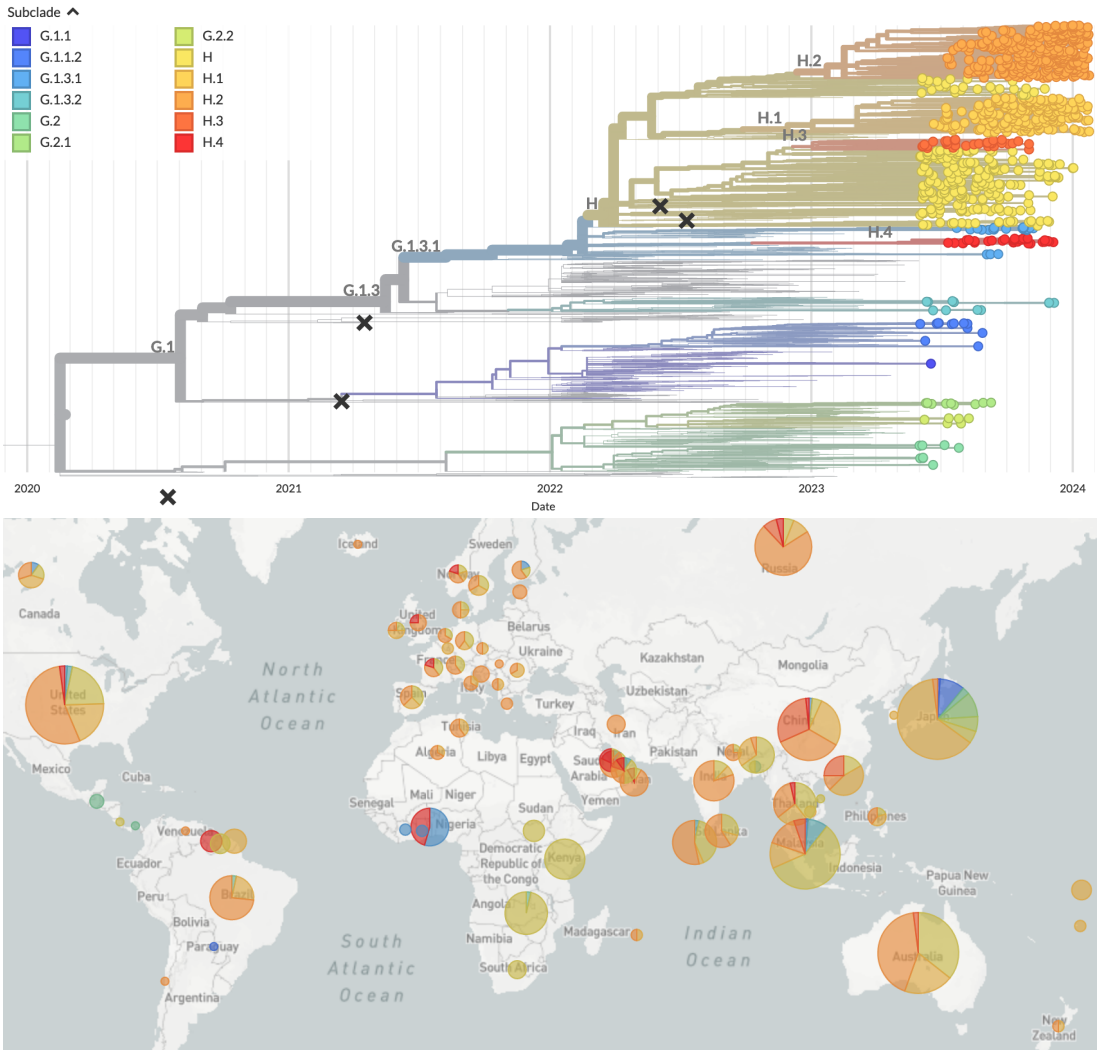

Figure 9. Time-resolved A/H3N2 phylogeny colored by clade and filtered to strains collected since June 1, 2023 (top) and corresponding geographic distribution of strains shown in the phylogeny (bottom). View on nextstrain.org.

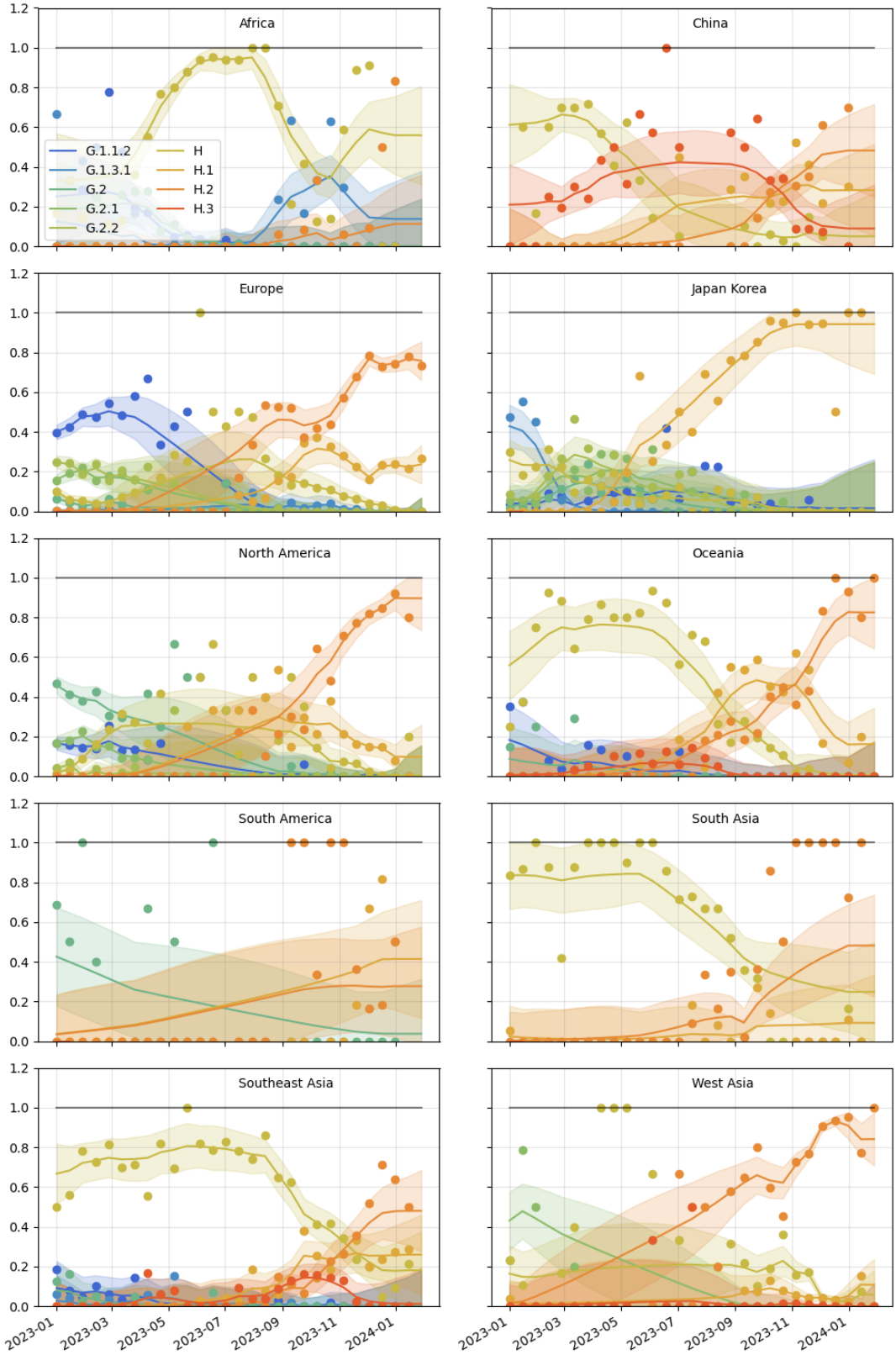

Figure 10. HA clade frequency dynamics in different regions of the world.

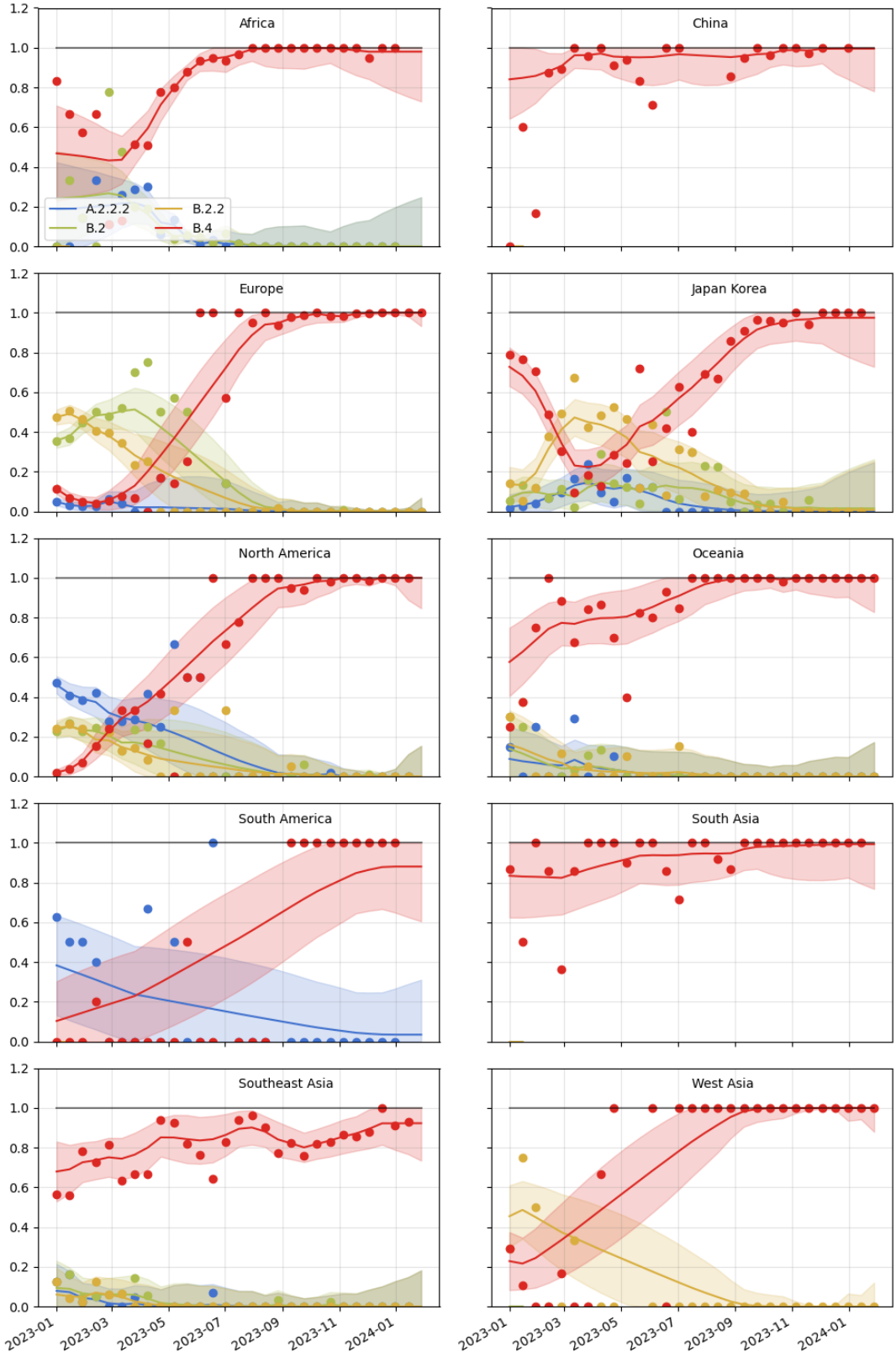

Figure 11. NA clade frequency dynamics in different regions of the world.

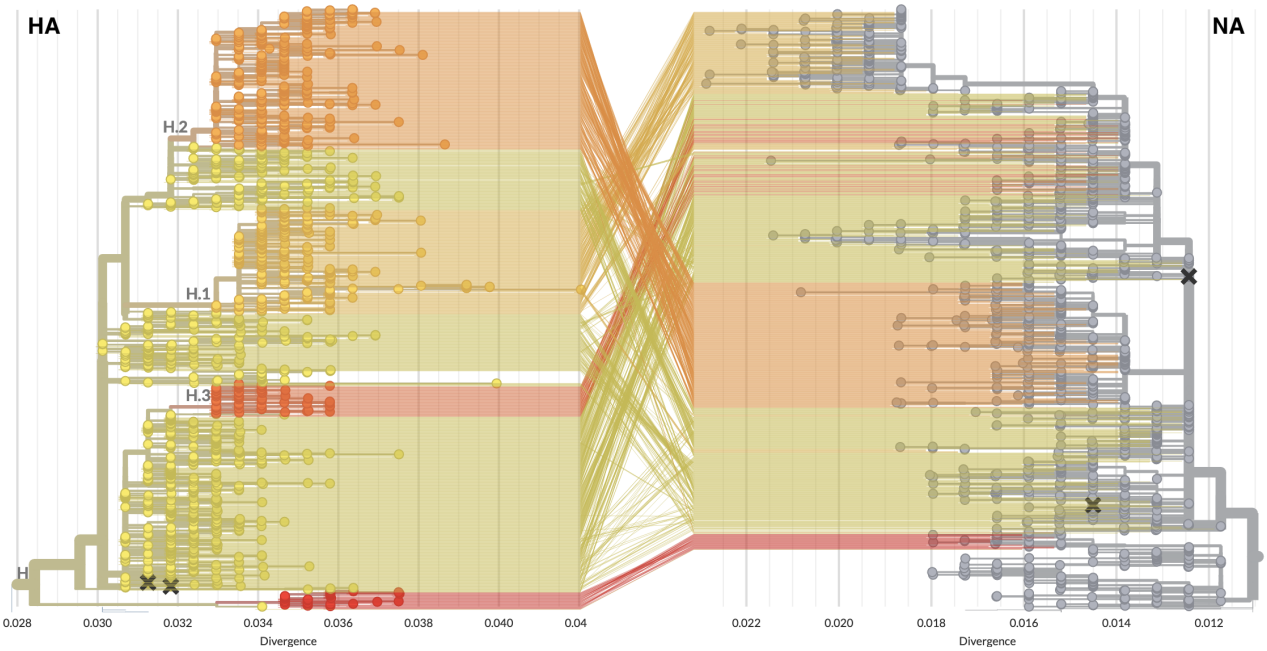

Figure 12. Tanglegram of A/H3N2 phylogenies for HA (left) and NA (right). HA clades H.1 and H.2 are associated with a different NA backgrounds. View on nextstrain.org.

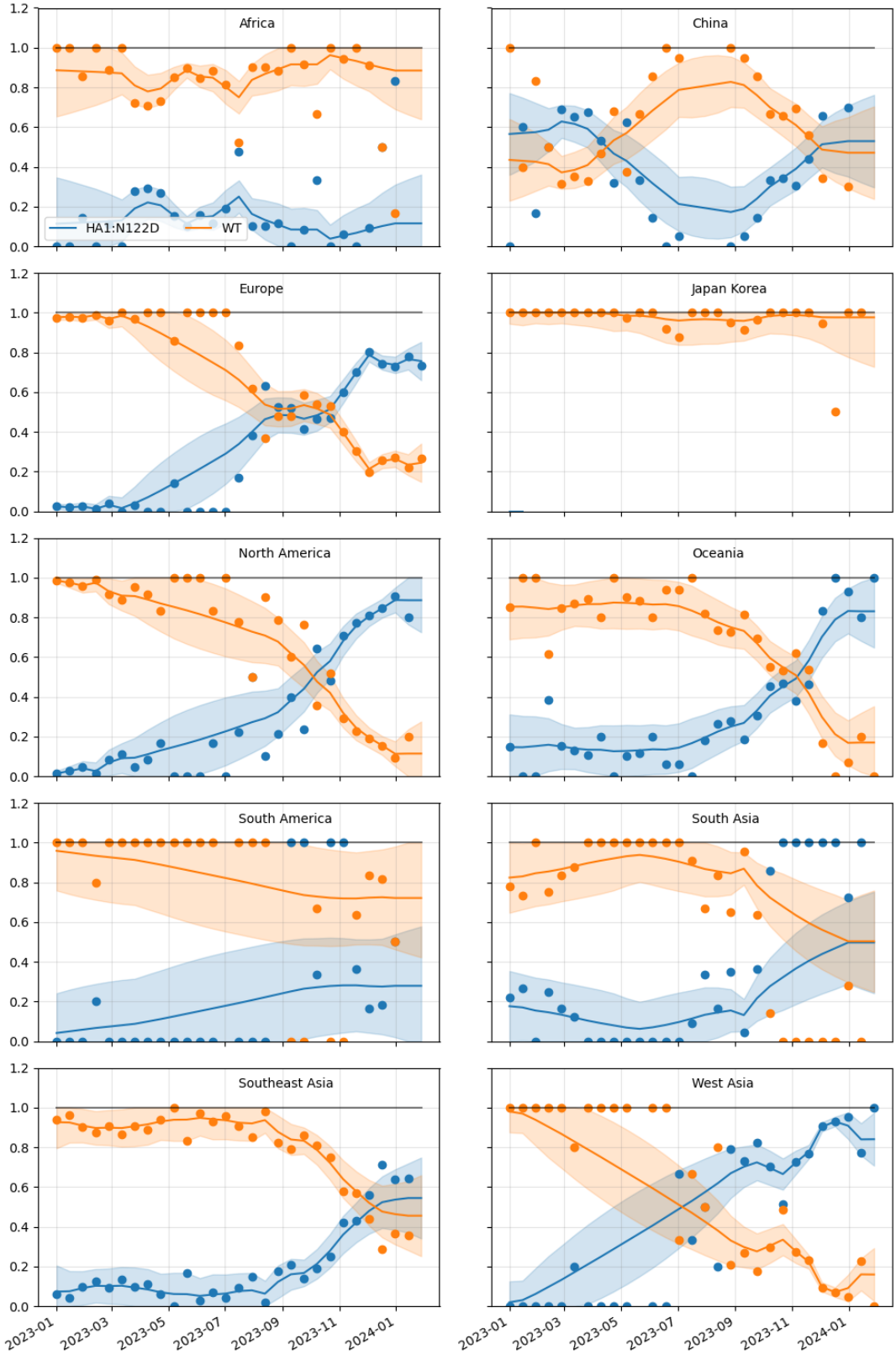

Figure 13. Frequency dynamics of substitutions at position 122 in HA1 in different regions of the world.

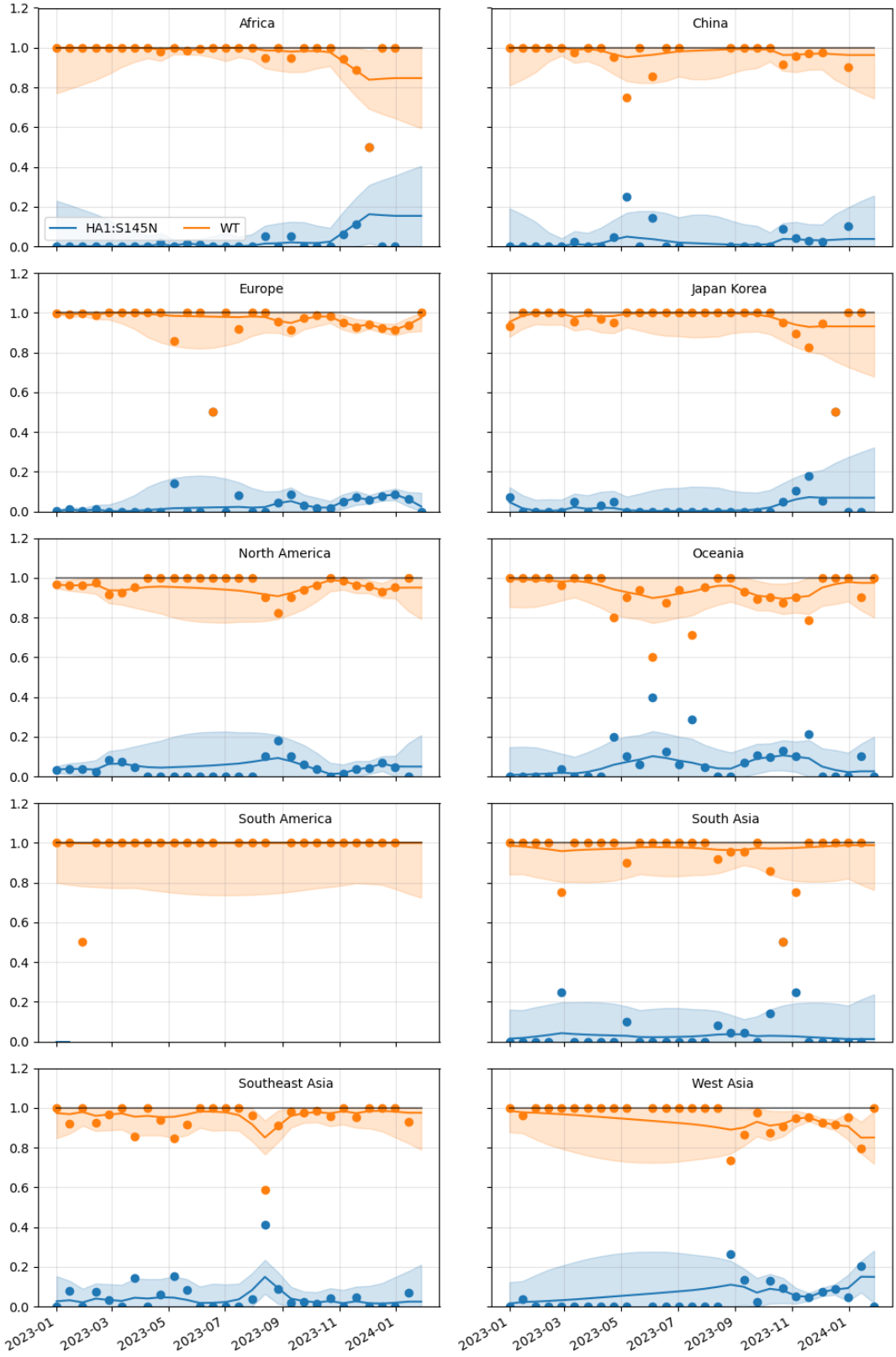

Figure 14. Frequency dynamics of substitutions at position 145 in HA1 in different regions of the world.

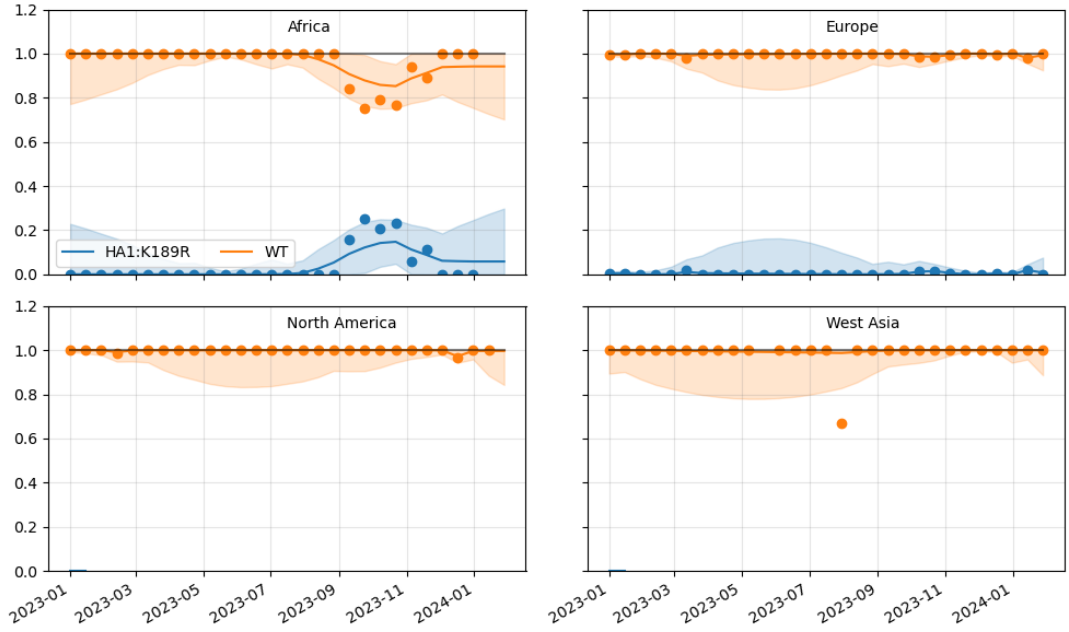

Figure 15. Frequency dynamics of substitutions at position 189 in HA1 in different regions of the world.

Antigenic properties from ferret serology

We integrated FRA/VN/HINT data from the WHO Collaborating Centers in London, Tokyo, Melbourne, and Atlanta with molecular evolution of the HA segment. The current northern hemisphere vaccine, A/Darwin/6/2021, effectively covers clade H and its descendants H.1, H.2, and H.3. The new southern hemisphere vaccine, A/Massachusetts/18/2022, covers clades H, H.1, and H.3, but recent H.2 strains have an average $\log_2$ distance greater than 1 indicating drift from sera against the Massachusetts/18 strain. The clade H reference strain A/NewYork/66/2022 has the HA1:122D substitution associated with a loss of glycosylation and shows an average antigenic distance from H.2 strains of less than 1 $\log_2$ units. The different between titer drops of H.2 compared to H and H.1 strains is similar with and without the HA1:122D substitution.

A/Sydney/878/2023 descends from the H.2 clade and covers H.2, H.1, and H equally well. Among the egg-passaged vaccines, A/Darwin/9/2021-egg shows the lowest average antigenic distance from H and H.1 strains of about 1. A/Thailand/8/2022-egg poorly covers recent H.2 strains with an average distance greater than 2 $\log_2$ units.

In HI-based assays with cell-passaged data the K276E substitution defining clade H.2 seems to have stronger effect than in FRA based assays. Specifically, HI measurements using sera raised against A/Massachusetts/18/2022, A/Thailand/8/2022, and A/SouthAustralia/48/20223 show a 4-fold titer drop for recent H.2 strains. This drop is less pronounced for A/NewYork/66/2022.

Assays with sera raised against A/Darwin/6/2021 show a 2-fold titer drop for recent strains in H compared to the FRA measurements, but don't seem to differentiate much between H and H.2. In contrast, sera against A/Sydney/878/2023 from H.2 appears to cover H, H.1, and H.2 similarly well. None of the egg-passaged candidates show effective coverage of recent H.2 strains in HI measurements.

Antigenic properties from pooled human sera

To estimate the effects of recent mutations on human immune responses, we plotted titer measurements from pooled human sera against recently circulating test viruses using the Nextstrain measurement panel [7]. Sera came from humans who had been recently vaccinated in the 2022/2023 season with a cell-passaged A/Darwin/6/2021. We analyzed data from FRA and HI assays with cell-passaged test strains, focusing on measurements collected since June 1, 2023 for test viruses descended from clade G (2). Post-vaccination sera against A/Darwin/6/2021 similarly covered recent clades in both assay types including effective coverage of clade H and its descendants.

Antigenic properties from deep mutational scanning experiments with human sera

Frances Welsh, a PhD student in Jesse Bloom's lab, recently produced deep mutational scanning with mutations in the HA background of A/HongKong/45/2019 (A/H3N2) and measured how well mutations escaped antibodies from 28 sera from individuals of different ages spanning children to older adults. These results were shared in December via a preprint on bioRxiv [8]. In brief, this method generates a diverse library of HA sequences with single amino acid mutations on the HK19 background, propagates the virus in presence or absence of sera, and then compares the frequencies of specific substitutions in the two experiments using deep sequencing and quantified as an escape score that correlates well with inhibition titers. This method can reveal escape mutations as well as sensitizing changes, see Fig. 16.

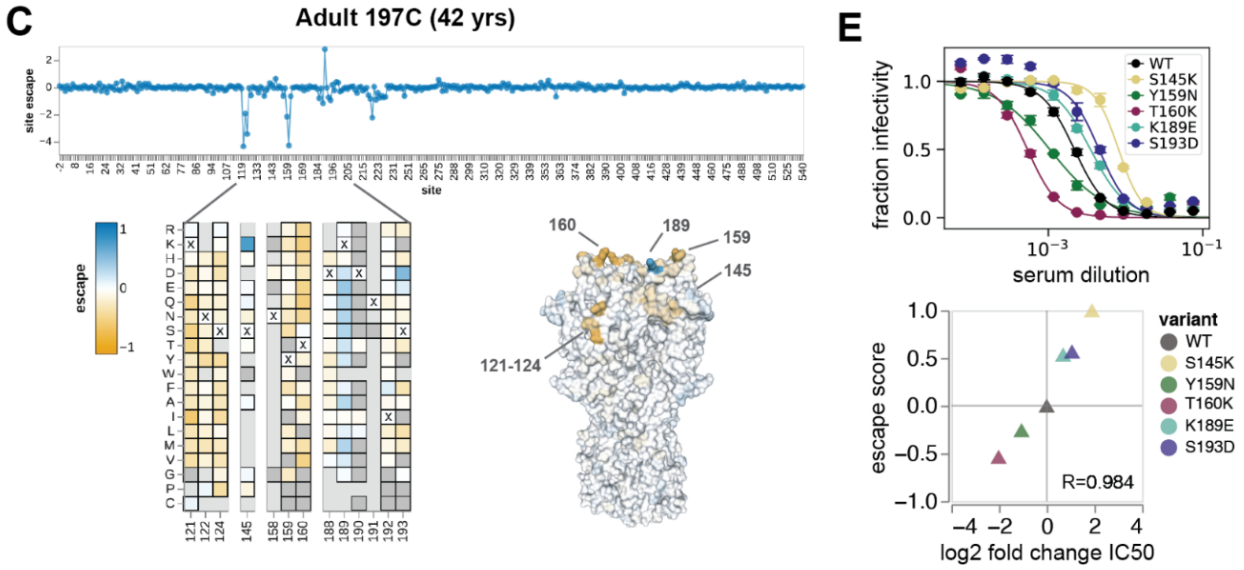

Figure 16. Escape scores for mutations on the A/HongKong/45/2019 (A/H3N2) background in the presence of serum from an adult. For this indivual, the summary along the HA1 protein reveals sensitizing mutations around positions 121-124 and 159/160, as well as escape mutations at postions 145, 189, and 193 (note that the aggregate escape score exaggerates the contributions of sites with many permissive escape mutations.). The two panels on the right show the concordance of the DMS score with fold-change in inhibition titer for the same mutations. (From Figure 1 in [8])

Across sera, HA1 sites 50, 82, 124, 135, 137, 143, 144, 145, 157, 159, 189, 193, 275, 276 where often found to lead to escape. Interestingly, positions 193, 159, and 50 have swept since 2019 and now 276

and 144 are increasing in frequency, suggestion that these data would have been predicitive in the years 2020-2023. HA sequences have changed substantially since A/HongKong/45/2019 and it is unclear how predicitive these escape scores are of future evolution. Fig. 17 shows the escape score per clade highlighting genotypes at positions 144, 145, and 189. H.2 has the highest average escape score, but additional mutations at the highlighted positions can elevate the escape score substantially across subclades of H.

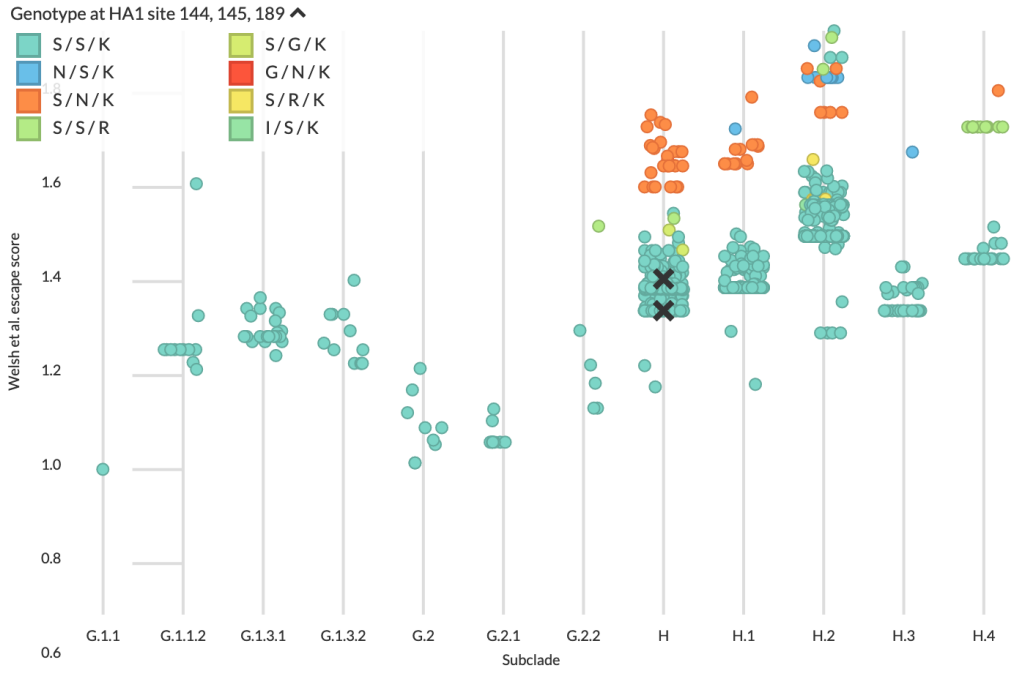

Figure 17. Escape score from Welsh et al. data per clade [8] by clade. Each point represents a single HA sequence plotted by cumulative escape score on the y-axis, clade on the x-axis, and colored by genotype at HA1 positions 144, 145, and 189. View on nextstrain.org.

Fitness estimates

H clades have the highest local branching index (LBI) values by far, corresponding to their rapid recent growth (Fig. 18). Among them, H.2 has the highest LBI due to its recent expansion.

We estimated the fitness of currently circulating strains based on a combination of mutational load from non-epitope mutations and either antigenic novelty based on FRA data or recent population growth based on the local branching index (LBI). We previously trained models based on these fitness metrics that minimized the distance between observed and predicted populations one year in the future [6]. In our comprehensive testing, the most reliable forecasts combined fitness metrics for mutational load and either antigenic novelty or LBI. These validated models forecast the future frequency of H3N2 clades. For the first time, we also include a simple forecasting model based on Welsh et al. escape scores described above. The predictions below should therefore be interpreted carefully.

We generated five H3N2 HA tree replicates and corresponding forecasts for a) the antigenic novelty model based on ferret cell FRA data, b) the antigenic novelty model based on human cell FRA data, c) local branching index, and d) Welsh et al. escape scores (Fig. 19). Both antigenic novelty models predict the growth of clade H.1 and corresponding decline of H.2. Antigenic measures of our fitness

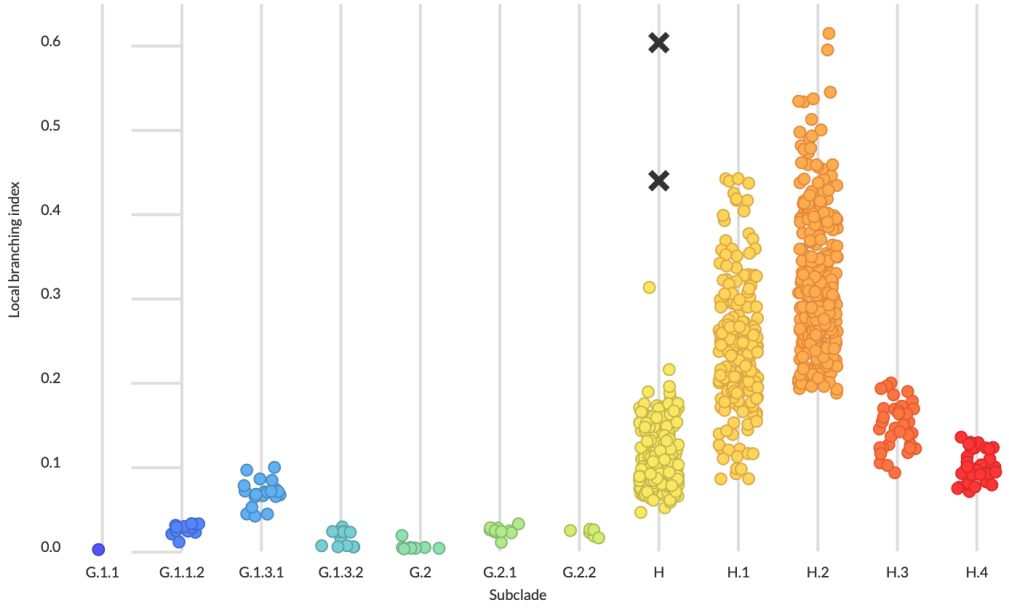

Figure 18. Local branching index per clade [5]. View on nextstrain.org.

model penalize clades that have circulated recently at higher frequency, and thus both antigenic models currently favor the lower frequency clade H.1. In contrast, the models based on either LBI or Welsh et al. escape scores both predict the continued growth and eventual fixation H.2. These latter predictions correspond to the higher LBI (Fig. 18) and escape scores (Fig. 17) associated with H.2 compared to H.1. In recent years, our antigenic model has been problematic and we have higher confidence in the LBI and escape score models. Neither H.3 nor H.4 are predicted to grow substantially under any of the models.

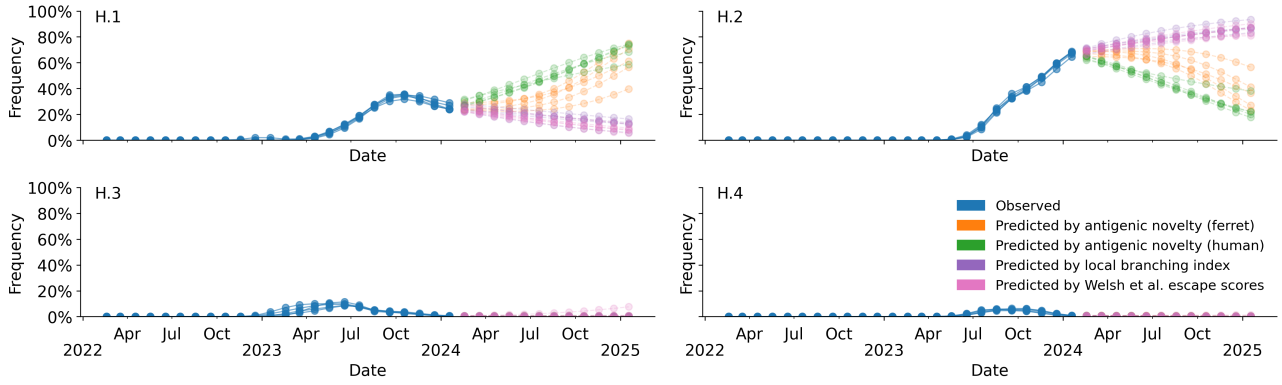

Figure 19. Observed and predicted clade frequencies for all extant clades descending from clade H based on forecasts from five replicates of four models including a) antigenic novelty based on ferret serology, b) antigenic novelty based on human serology, c) local branching index, and d) Welsh et al. escape scores.

B/Vic

In the last six months, B/Victoria has been sequenced primarily in North America. Sequence counts remain relatively low compared to the peak season in Europe last February and March. Clade C.5 has nearly fixed globally and diversified into subclades including several with recurrent HA1:197E and HA1:183K substitutions. The current vaccine strain, B/Austria/1359417/2021 (basal in C), continues to effectively cover clade C strains observed in the last year.

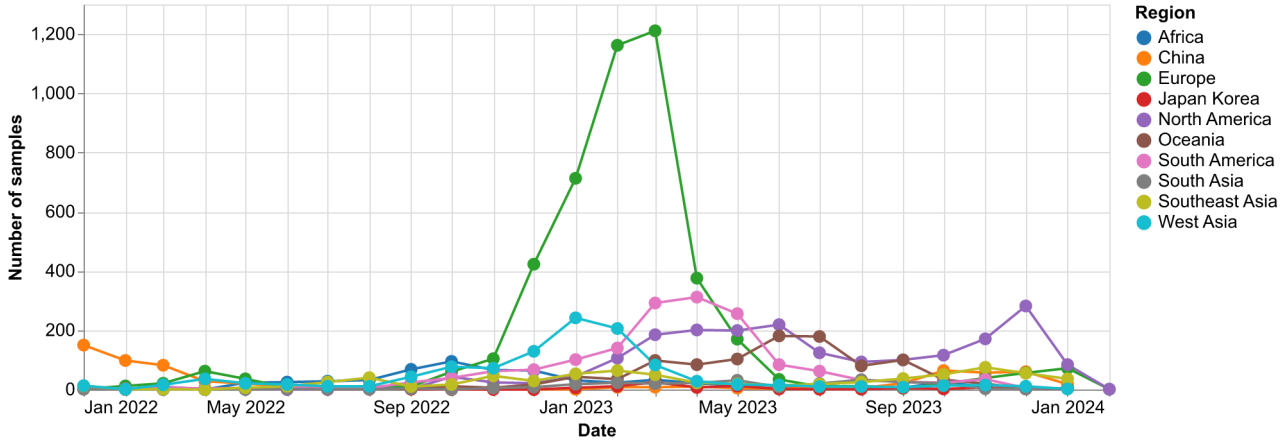

Figure 20. Sample counts through time and across regions.

Current circulation patterns

B/Vic has been continuously observed in North America in the last year, while its appearance in other regions has varied (Fig. 20). All recent strains descend from the clade C (V1A.3a.2) with most of the diversity descending from the clade C.5 which carries a HA1:197E substitution (Fig. 21). Unlike H1N1pdm and H3N2, most of B/Vic diversity has circulated in most of the world in the last year. No single clade has dominated globally, but some clades show signs of fixing in specific regions. C.5.1 is growing rapidly in North America, while C.5.7 is at high frequency in China (Fig. 22). C.5.6 and C.5.7 appear to be growing in Europe, Oceania, South Asia, Southeast Asia, and West Asia. However, sequence counts remain low in most regions, so fitness dynamics between clades are not clear.

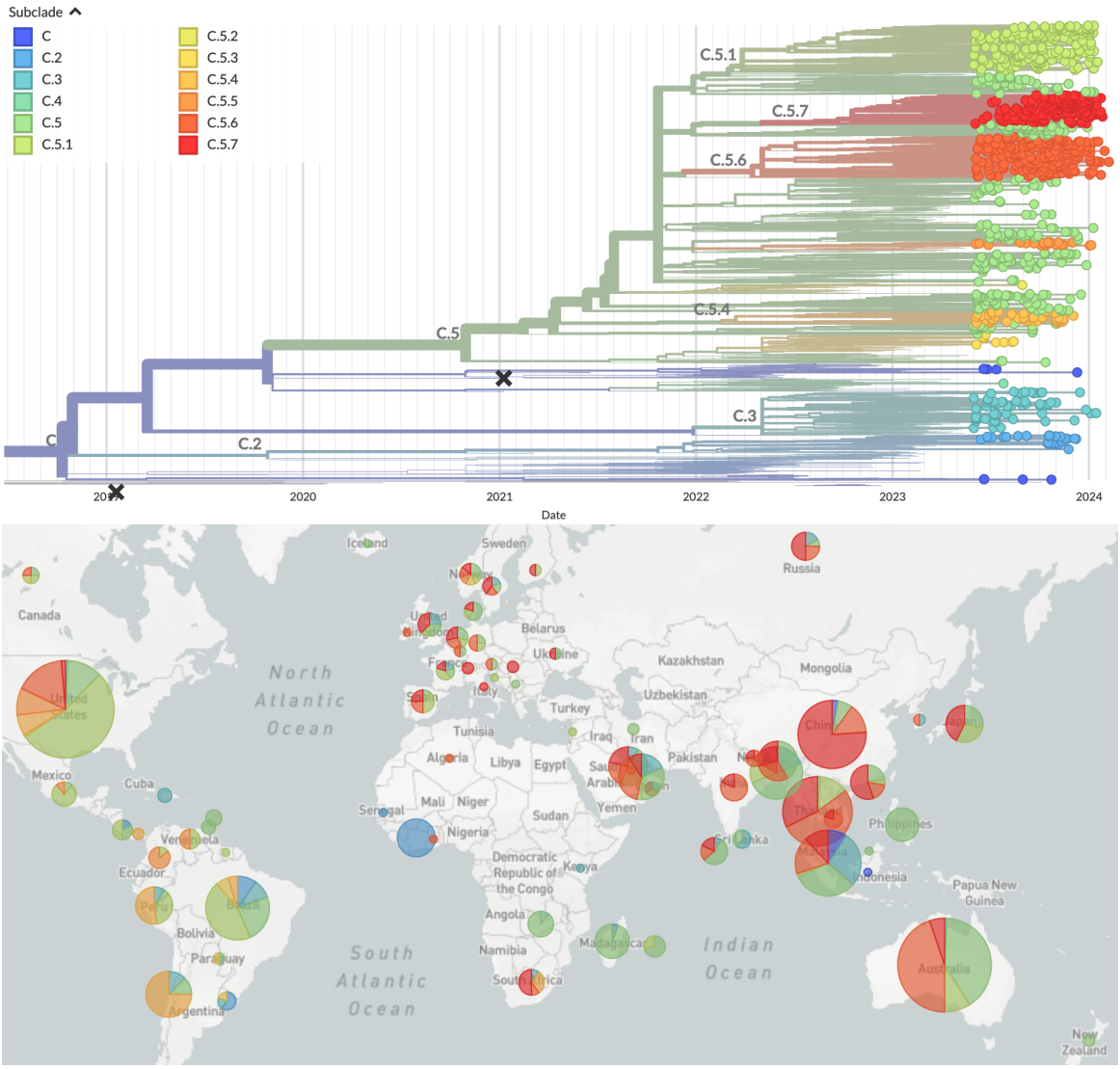

Figure 21. Time-resolved B/Victoria phylogeny colored by clade and filtered to strains collected since June 1, 2023 (top) and corresponding country-level geographic distribution of strains shown in the phylogeny (bottom). View on nextstrain.org.

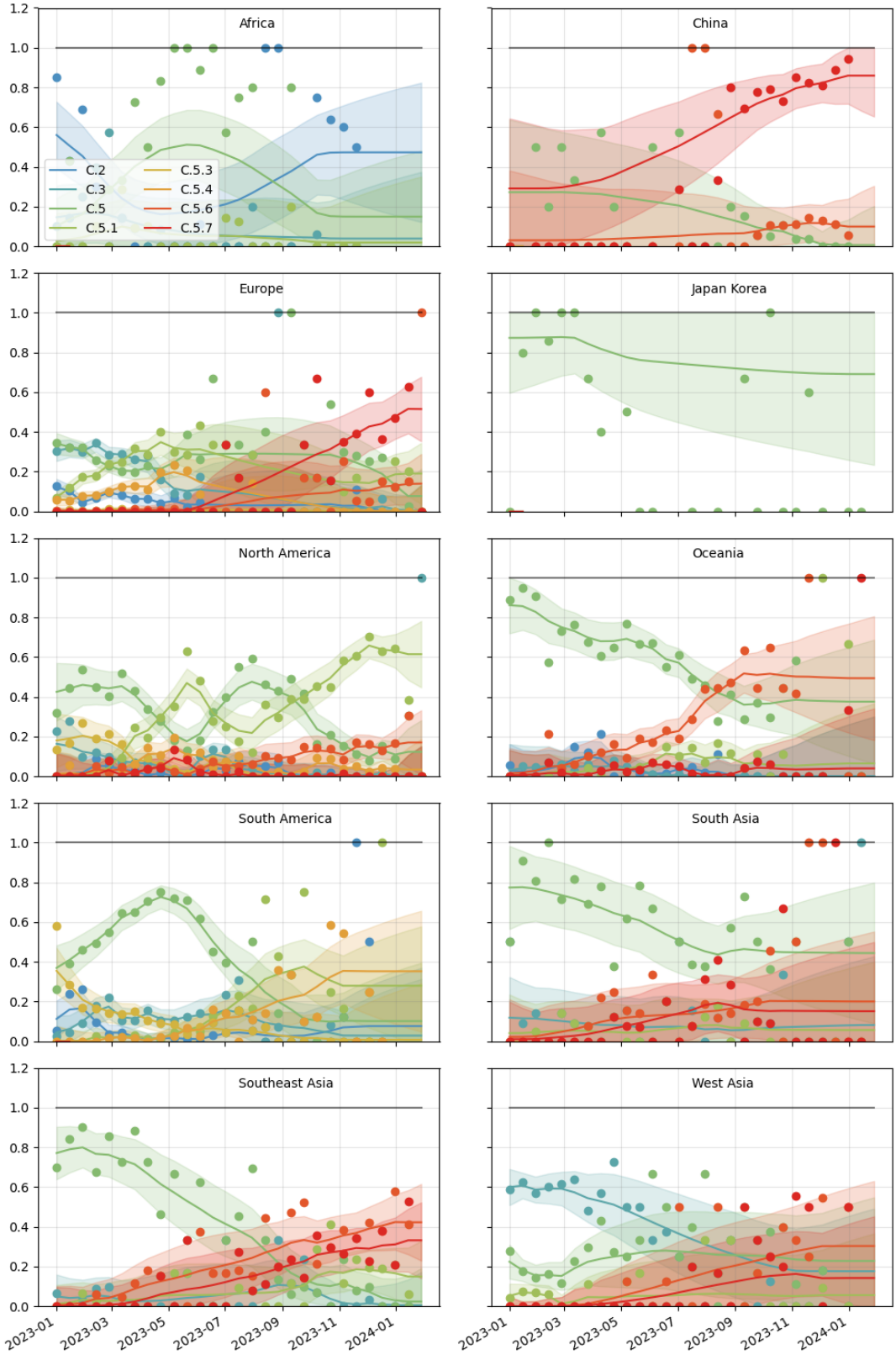

Figure 22. HA clade frequency dynamics in different regions of the world.

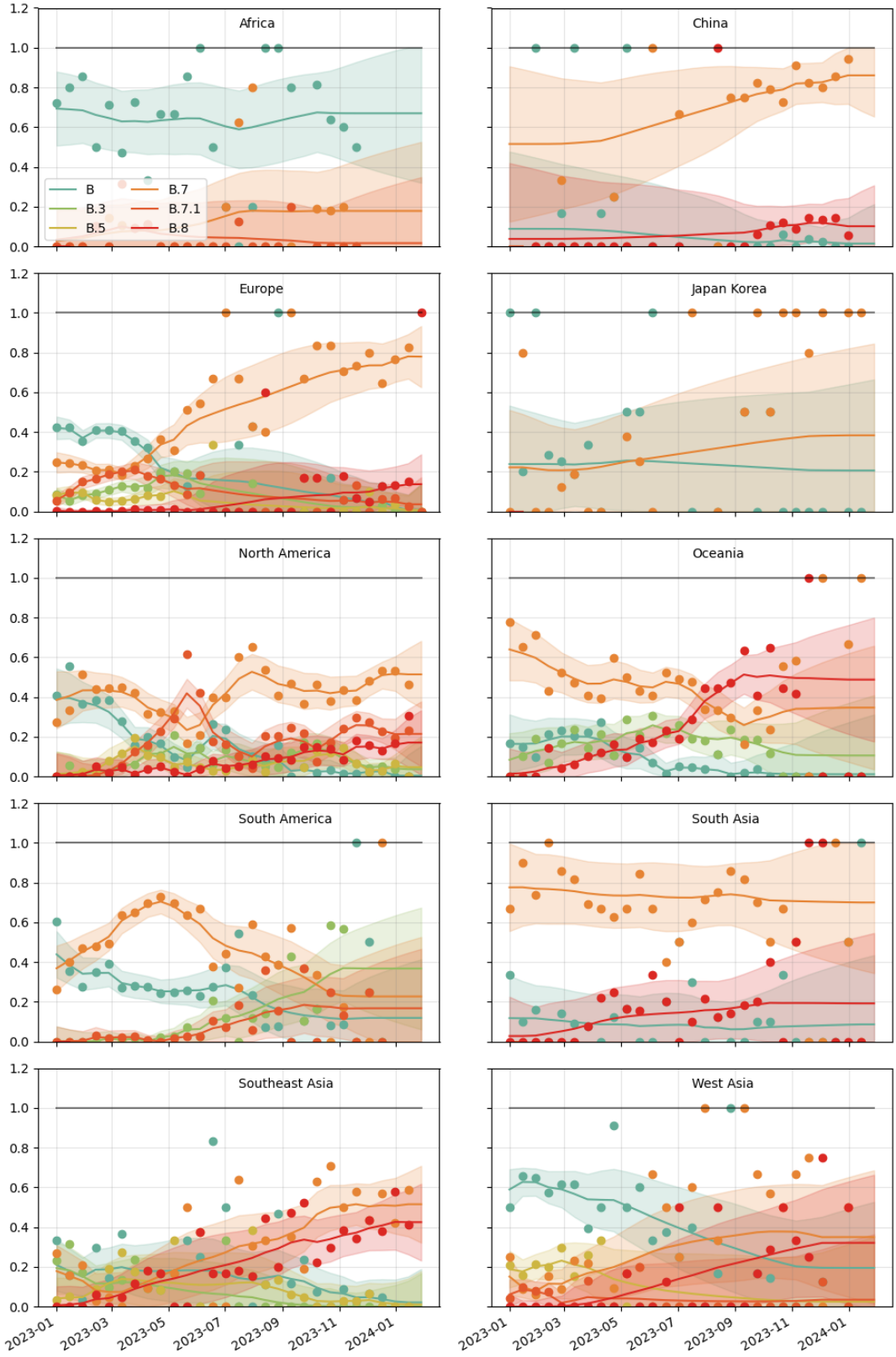

Figure 23. NA clade frequency dynamics in different regions of the world.

Antigenic properties

We integrated HI data from the WHO Collaborating Centers in London, Tokyo, Melbourne, and Atlanta with molecular evolution of the HA segment. Based on cell- and egg-passaged HI data, the current vaccine strain, A/Austria/1359417/2021, effectively covers recent clade C (3a.2) strains.

Fitness estimates

Vic clades show little variation in antigenic novelty (Fig. 24). However, clades C.5.6 and C.5.7 have some of the highest LBI values, followed by C.5.1 (Fig. 25).

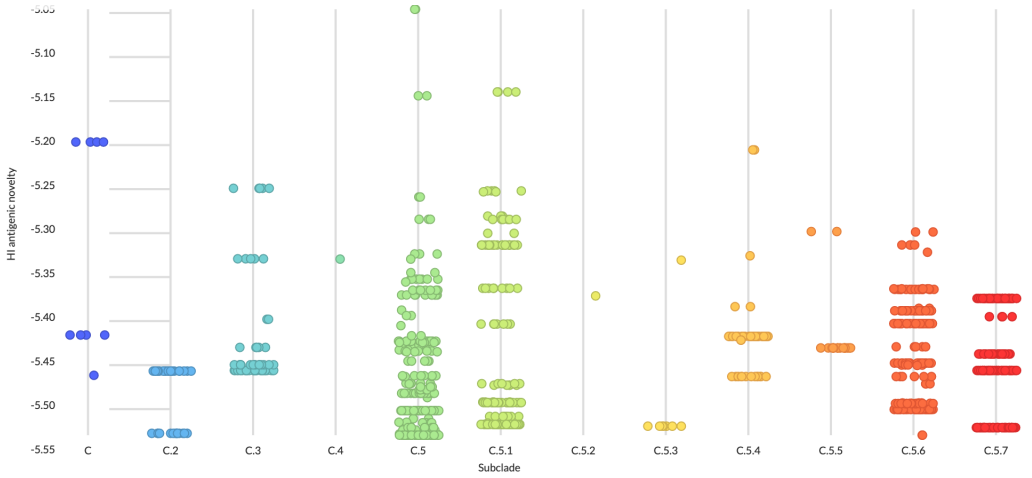

Figure 24. Antigenic novelty per clade estimated from ferret-based HI data [6] for samples collected since June 1, 2023. View on nextstrain.org.

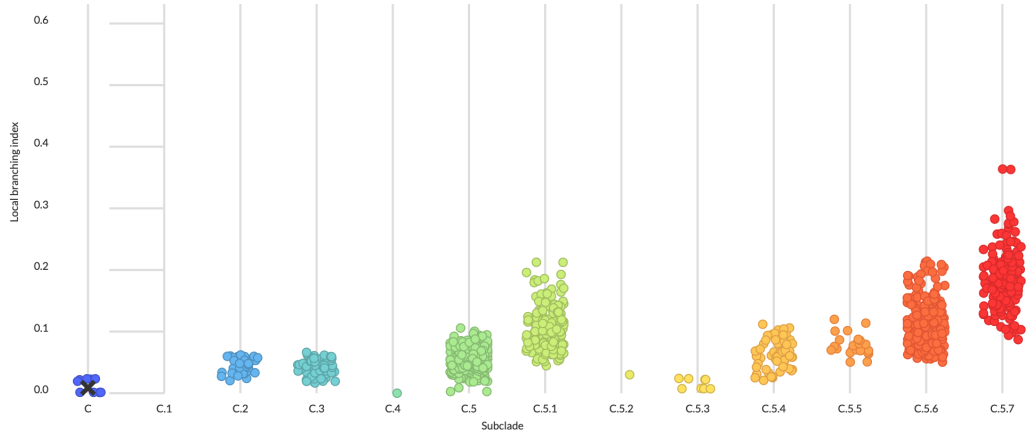

Figure 25. Local branching index per clade [5] for samples collected since June 1, 2023. View on nextstrain.org.

Acknowledgments

This work is made possible by the timely sharing of influenza virus sequence data through GISAID. A table acknowledging each individual data contributor to the analysis on nextstrain.org/flu can be found online at nextstrain.org/flu. We thank the Influenza Division at the US Centers for Disease Control and Prevention, the Victorian Infectious Diseases Reference Laboratory at the Australian Peter Doherty Institute for Infection and Immunity, the Influenza Virus Research Center at the Japan National Institute of Infectious Diseases, the Crick Worldwide Influenza Centre at the UK Francis Crick Institute, Jesse Bloom and his lab, for data sharing and feedback. We thank David Wentworth, Rebecca Kondor and Vivien Dugan for insight regarding analysis directions.

References

1. Neher RA, Bedford T (2015) nextflu: real-time tracking of seasonal influenza virus evolution in humans. Bioinformatics 31: 3546–3548.
2. Hadfield J, Megill C, Bell SM, Huddleston J, Potter B, et al. (2018) Nextstrain: real-time tracking of pathogen evolution. Bioinformatics 34: 4121–4123.
3. Aksamentov I, Roemer C, Hodcroft EB, Neher RA (2021) Nextclade: clade assignment, mutation calling and quality control for viral genomes. Journal of Open Source Software 6: 3773.
4. Neher RA, Bedford T, Daniels RS, Russell CA, Shraiman BI (2016) Prediction, dynamics, and visualization of antigenic phenotypes of seasonal influenza viruses. Proc Natl Acad Sci USA 113: E1701–E1709.
5. Neher RA, Russell CA, Shraiman BI (2014) Predicting evolution from the shape of genealogical trees. eLife 3: e03568.
6. Huddleston J, Barnes JR, Rowe T, Xu X, Kondor R, et al. (2020) Integrating genotypes and phenotypes improves long-term forecasts of seasonal influenza A/H3N2 evolution. eLife 9: e60067.
7. Lee J, Hadfield J, Black A, Sibley TR, Neher RA, et al. (2023) Joint visualization of seasonal influenza serology and phylogeny to inform vaccine composition. Front Bioinform 3: 1069487.
8. Welsh FC, Eguia RT, Lee JM, Haddox HK, Galloway J, et al. (2023) Age-dependent heterogeneity in the antigenic effects of mutations to influenza hemagglutinin. bioRxiv .